

The Wealth of Information from Transient Guest Profiles

*Tomas Binder, Christian Chmelik, Lars Heinke, Florian Hibbe, Jörg Kärger,
Tobias Titze, Despina Tzoulaki*

Universität Leipzig, Fakultät für Physik und Geowissenschaften, Germany
Corresponding author: Jörg Kärger, kaerger@physik.uni-leipzig.de

Abstract

The application of interference microscopy (IFM) and infrared microscopy (IRM) to monitor the evolution of the concentration of guest molecules in nanoporous host materials opens a new field of diffusion research in condensed matter. It combines the methodical virtues of the profiling methods of solid-state diffusion studies with the benefit of the mobility enhancement in fluids. We are going to illustrate the rich options of diffusion studies provided by this novel experimental approach.

Keywords: Nanoporous materials, diffusion, profiling, permeability, IR microscopy, interference microscopy, tracer techniques, surface resistances, zeolites, metal-organic frameworks

1. Introduction

Not unlike other research areas in science, the history of diffusion is accompanied by a continuous accomplishment of the measuring techniques, ranging from ensemble measurement to single-particle studies. Following 150 years of ensemble measurement in mainly fluids, the first recording of single-particle diffusion by Perrin provided nothing less than the ultimate proof of the atomistic structure of matter [1]. In parallel, profiling techniques, i.e. techniques to record the evolution of the distribution of the constituents, with fluids (notably by optical techniques [2]) and with solids (notably with tracer techniques [3]) attained increasing importance. The introduction of nuclear magnetic resonance with pulsed field gradients [4, 5] enabled the measurement of the averaged "propagator" [6], i.e. of the probability distribution of displacements within the entity of guest molecules within a sample. The propagator comprehensively characterises an ensemble of randomly moving molecules and represents a key-quantity in "dynamic micro-imaging" [4, 5, 7], i.e. in the exploration of the structural features of complex systems via their diffusion properties [8]. More recently, single particle tracking with sub-diffraction resolution (see also the contribution by Bräuchle and co-authors to this volume) opened new routes to a better understanding of the functionality of living organisms [9] and has successfully been applied to tracing the channel architecture in nanoporous materials [10].

With the application of infrared microscopy (IRM, also referred to as IR micro-imaging [11-13]) and interference microscopy (IFM [11, 13-15]) to monitor the concentration profiles in nanoporous materials, most recently a novel opportunity of studying diffusion phenomena has been opened up. With this contribution we would like

to visualize the novel level of information which, in some key issues of diffusion research, notably exceeds the possibilities which so far have been accessible.

2. Techniques of Measurement

2.1. Interference microscopy (IFM)

Following its application to fluids [2, 16], optical interference techniques, in particular interference microscopy (IFM), has recently been introduced to diffusion studies on microporous materials [11, 13-15, 17-19]. A schematic representation of its instrumentation is provided by Fig. 1. The high spatial resolution ($0.5 \times 0.5 \mu\text{m}^2$) and the ability to monitor the evolution of intracrystalline concentration profiles make this method a unique tool for exploring transport phenomena in nanoporous host-guest systems, as an ideal model system for the visualization of diffusion patterns quite in general. It is worthwhile mentioning that the option of this type of measurement has been suggested and probed in preliminary studies already three decades ago (see [20] and pp. 214-215 of [21]). However, it was only the further technical accomplishment of the *Jenamap p dyn* series of interference microscopes by the Carl Zeiss Jena GmbH and the introduction of powerful computers and data analysis [17, 22, 23] that, eventually, enabled the measurement of transient intracrystalline concentration profiles.

Prior to the measurements, the cell with crystals is “activated”, i.e. heated up and kept under vacuum, in order to remove the impurities from the pore system. Afterwards, after cooling down to the temperature of measurement, the sample is brought into contact with the atmosphere of the probe gas, which is thus introduced as a “guest” into the sample, i.e., into the “host” material. By variation of the gas pressure in the surrounding gas atmosphere, molecular uptake or release is initiated. The camera on top of the microscope records the interference pattern of the crystal under study. In our present device, the minimum time interval between (two) subsequent profiles is of the order of 10 s. Presently, this time interval is needed to unambiguously transfer the interference patterns to the corresponding phase shifts. Further methodical development will diminish this limit into the range of seconds [19].

The technique is based on the analysis of the interference pattern generated by the superposition of two light beams, one passing through the nanoporous crystal and the other passing through the surrounding atmosphere. Since the optical density depends on the concentration of the guest molecules, changes in local concentration appear directly as corresponding changes in the interference patterns. Therefore, it is possible to deduce the concentration profiles from the measured changes in the interference pattern. The quantity directly accessible is the integral over the intracrystalline concentration in the observation direction with a spatial resolution of $\Delta y \times \Delta z \approx 0.5 \mu\text{m} \times 0.5 \mu\text{m}$. If, due to a corresponding blockage of the relevant crystal faces or because of the architecture of the pore system, diffusion in the x -direction is prohibited, there will be no variation of concentration in that direction. In this case, interference microscopy directly yields the local concentrations $c(y,z)$. Otherwise, a more complex analysis must be used for studying the mass transfer [24].

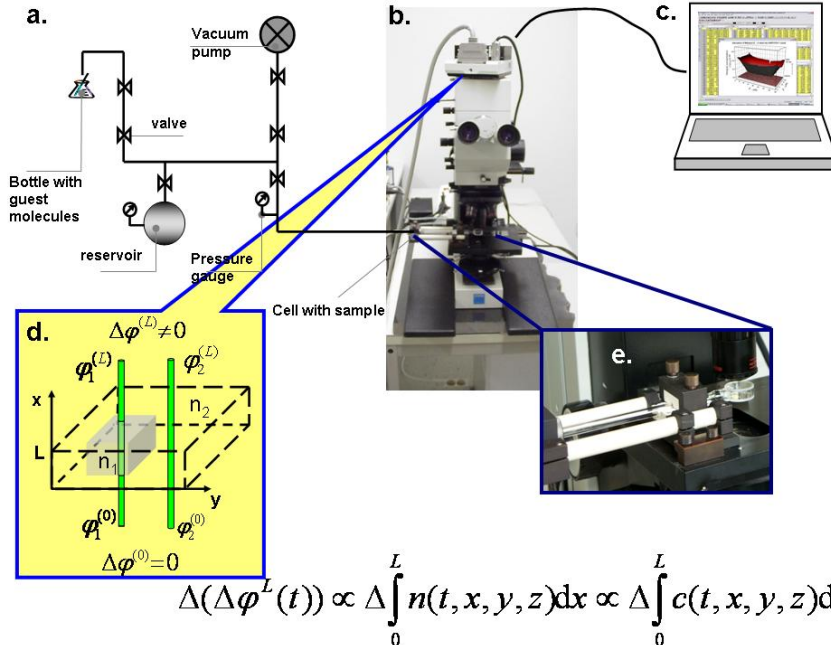


Fig. 1: Schematics of the application of interference microscopy (IFM) for monitoring transient intracrystalline concentration profiles: (a) A schematic representation of the vacuum system to which the cell with the sample is attached; (b) The interference microscope on top of which the camera is placed; (c) The computer which is directly connected to the camera; (d) A schematic representation of the principle of the technique: changes in the intracrystalline concentration during diffusion of guest molecules will affect the refractive index of the crystal (n_1) and, hence, the phase difference $\Delta\phi$ of the two beams. The correlation of these variables is reflected by the mathematical relation of the figure. Having measured the difference of the optical path length we can evaluate the difference of the intracrystalline concentration; (e) Enlarged view of the cell containing the crystal under study.

2.2. Infrared microscopy (IRM)

Guest concentrations in nanoporous crystals can be directly monitored by using the molecular property to absorb infrared (IR) light of well-defined wave lengths. Today, wave length analysis is generally based on Fourier transformation (FT). Detailed information about the principles of FTIR spectroscopy may be found in the literature [25-30]. We use an FTIR microscope of type Bruker Hyperion 3000 consisting of a spectrometer (Bruker Vertex 80v) and a microscope with a Focal Plane Array (FPA) detector (Fig. 2) [11, 13, 31, 32]. The novel FPA detector consists of an array of 128×128 single detectors with a size of $40 \mu\text{m} \times 40 \mu\text{m}$ each. By means of a 15x objective, a resolution of $2.7 \mu\text{m} \times 2.7 \mu\text{m}$ is gained in the focal plane, where the crystals are placed.

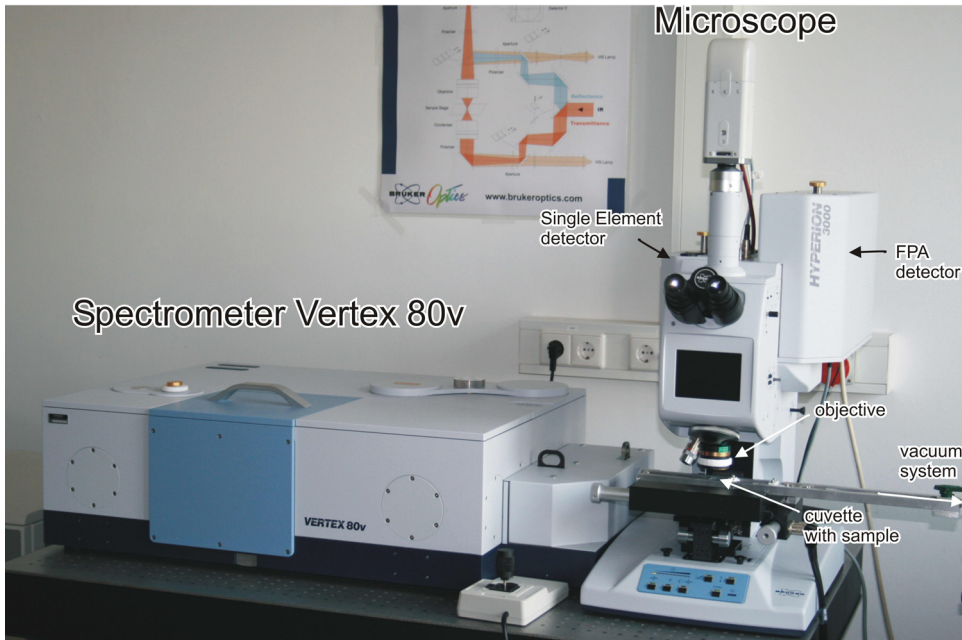


Fig. 2: IR micro-imaging device Bruker Hyperion 3000, consisting of a spectrometer and the microscope, with optics and detectors. The main part of the spectrometer is a Michelson interferometer.

Each single element of the FPA detector records an IR signal. The intensity of the IR light as a function of the wavelength, i.e. the transmission spectrum, is determined by means of the spectrometer using Fourier transformation [25]. According to Lambert-Beer's law, the concentration of a particular molecular species is proportional to the intensity of the "absorption band", defined as the negative logarithm of the ratio between the transmission spectrum of the sample over the relevant frequency range and of the corresponding background signal [25]. By comparison with a standard, also information about the absolute number of molecules becomes attainable.

Thus, IRM turns out to be really complementary to IFM. Offering a notably poorer spatial resolution (of the order of $3 \mu\text{m}$ in comparison with $0.5 \mu\text{m}$ as accessible by IFM), IRM is able to differentiate between different molecular species (using the resonance frequencies as a "finger print" for the different molecules) and, moreover, to provide absolute numbers of molecular concentrations, by comparison with a standard.

Figure 3 illustrates the three stages of concentration profiling by IRM, namely recording of the spectra (for each individual pixel, Fig. 3a), plotting of the intensity of a characteristic absorption band (being proportional to the molecular concentrations) over all pixels (Fig. 3b) and plotting of the concentration profiles along a certain line of interest across the host system under study (Fig. 3c).

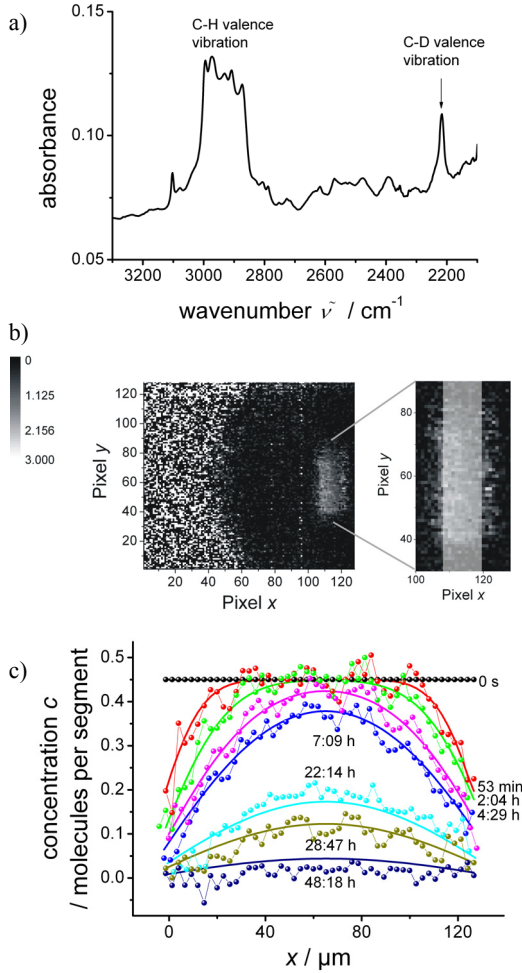


Fig. 3: Concentration profiles recorded with IR micro-imaging.

a) IR absorption spectra of deuterated propane in MOF Zn(tbip). The absorption band of the C-D valence vibrations is clearly distinguished from the band of the C-H valence vibrations of the crystal framework.

b) Two-dimensional profile of the C-D absorption band recorded by IR micro-imaging. The gray scale displays the intensity of the C-D band (from 0 to 3 a.u.). The crystal is equilibrated with a surrounding atmosphere of 60 mbar of deuterated propane. The bright bar represents the region which yields the profiles displayed in (c). The scattering on the left side of the picture is caused by a “corrupt” illumination of the detector caused by its large size.

c) Transient concentration profiles of deuterated propane in MOF Zn(tbip) during tracer exchange with the undeuterated isotope at an overall pressure of 60 mbar. The thin lines represent the best fits of the analytical solution (with constant diffusivity and permeability [33]) to the experimental data .

Following Hellmut Karge’s pioneering work in establishing IR microscopy as a technique of macroscopic [34] and mesoscopic [35] diffusion measurements, with the now available possibilities of IRM, also the direct observation of the evolution of concentration profiles inside the crystals – i.e. genuine “microscopic” [36, 37] diffusion measurements – have become possible [11, 13, 14], including the option of tracer exchange, i.e. of self- (or tracer) diffusion experiments. The steps leading to this type of experiment appear from Fig. 3.

Both IR micro-imaging and interference microscopy yield integrals over the concentration of the guest molecules in observation direction, as the primary data of the measurement. Hence, for hosts with channel systems in one or two dimensions, observation perpendicular to the channel direction directly yields the local concentrations. The examples we are going to discuss in the following will exactly refer to this type of host systems.

3. The Host Materials under Study

3.1. Zeolite ferrierite

Silica-ferrierite is a cation-free zeolite [38] with two perpendicular channel systems which intersect each other [39]. Fig. 4a) provides a schematic overview of the pore structure. One channel system is adjusted along y -direction and is framed by an 8-membered ring. This means that the rings around these channels are formed by 8 oxygen and 8 silicon atoms. The other channel system is along z -direction and consists of 10-membered ring channels. The outer geometry approaches a cuboid, with long sides in y - and z -direction ($L_y = 25 \mu\text{m}$ and $L_z = 100 \mu\text{m}$; l denotes the half-edge length) and a short-side length in x -direction ($l_x \approx 10 \mu\text{m}$). On both big-side faces of the crystal (parallel to y - z) there are small roof-like parts. The ferrierite crystals were activated under high vacuum at a temperature of 673 K for 12 h [40].

Due to large transport resistances at the entrances to the pores along z -direction in the crystal body, the mass transport proceeds mainly along y (Fig. 4b). As found out in ref. [40], the influence of the diffusion in z -direction increases with increasing pressure. Here, we analyse the release of methanol for a (small) gas pressure step from 10 mbar to vacuum, where the mass transfer proceeds (almost completely) one-dimensionally.

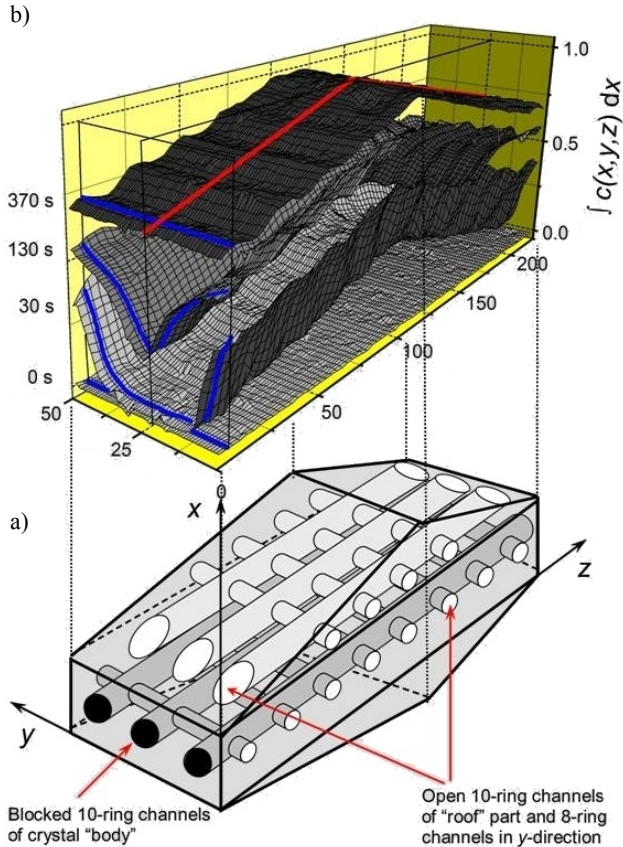


Fig. 4: Methanol in zeolite ferrierite.

a) Sketch of the ferrierite crystal with a two-dimensional pore structure in z - and y -direction. The scheme shows the cuboidal shape with the roof-like parts on the elongated side-faces.
 b) Two-dimensional profiles of the integral of the methanol concentration recorded by IFM during a pressure step from 0 to 80 mbar. The roof-like part is filled (almost) instantaneously. The mass transfer in the crystal body occurs mainly along y -direction.

3.2. Metal Organic Framework (MOF) Zn(tbip)

Zn(tbip) ($\text{H}_2\text{tbip} = 5\text{-tert-butyl isophthalic acid}$) [13, 41] is a highly stable representative of the family of metal organic frameworks (MOFs). The crystals are elongated, hexagonal prisms with lengths of hundreds and diameters of tens of micrometers. Zn(tbip) is traversed by an array of parallel chains of channel segments in the direction of longitudinal crystal extension (Figure 5). The resulting one-dimensionality of diffusion and the structural stability make MOFs of type Zn(tbip) excellent candidates for a systematic investigation of the mass transfer in nanoporous materials.

Prior to measurement, the sample was activated for 1.5 h under evacuation at 393 K. The adsorption isotherm was determined by means of IR microscopy and by means of Configurational-Bias Monte Carlo simulations [13].

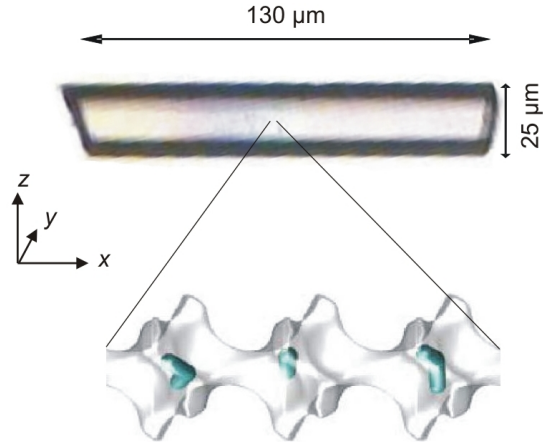


Fig. 5: Picture of an investigated Zn(tbip) crystal. The structure of the one-dimensional channel with a loading of 1 propane molecule per segment is also shown (adopted from [13]). The side pockets are ordered like two three-leaved clovers separated by windows of a diameter of 0.45 nm.

4. Novel Types of Experimental Evidence

4.1. Fast profile recording

Figure 6a displays the concentration profiles of methanol in the zeolite ferrierite after desorption onset by reducing the methanol pressure in the surrounding atmosphere from 10 mbar (corresponding to an initial loading of 1.9 molecules per nm³) to zero [40]. With such measurements of the dependence of the guest concentration $c(y,t)$ on space and time, both the guest molecule diffusivities D , and surface permeabilities α become accessible by direct (i.e. “in-situ” and “non-destructive”) observation. Both quantities are related to the flux density j which is the number of molecules passing a certain area in a given time interval, divided by this area and the time interval. The transport diffusivity is defined by Fick's 1st law

$$j = -D(c) \frac{\partial c(y,t)}{\partial y}. \quad (1)$$

The surface permeability of a given crystal face is the ratio between the flux $j(y=0, t) = j_{\text{surf}}$ through this face and the difference between the actual boundary concentration $c(y=0, t) = c_{\text{surf}}$ and the concentration established in equilibrium with the surrounding atmosphere of guest molecules (c_{eq}):

$$j_{\text{surf}} = \alpha(c_{\text{eq}} - c_{\text{surf}}). \quad (2)$$

Figure 6b displays the diffusivities and surface permeabilities computed using eqs. (1) and (2) and the concentration profiles in Fig. 6a. The consistency of this experimental approach is nicely reflected by the good agreement with the diffusivities and permeabilities observed in a second experimental run with a different pressure step. Note that this agreement does not only concern the order of magnitude in which the diffusivities are found. The measurements do even nicely reflect the whole functional

dependence of the surface permeabilities and of the diffusivities which, in these studies, cover more than one order of magnitude!

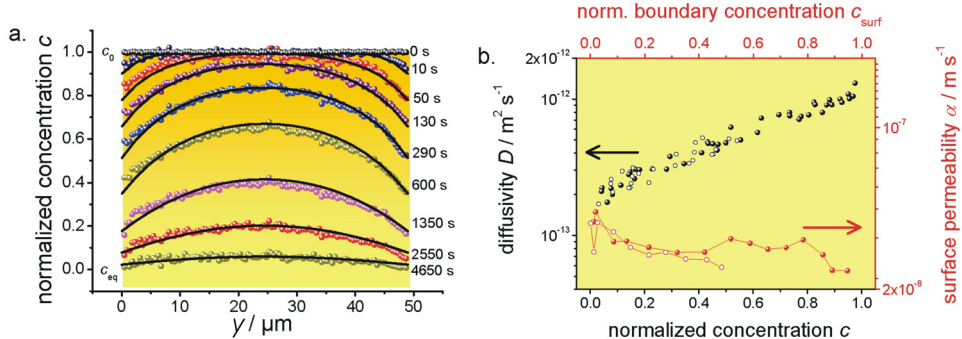


Fig. 6: Concentration profiles (a) and the resulting (transport) diffusivities and surface permeabilities (b) during methanol desorption from 10 mbar to 0 mbar in ferrirete. For comparison, fig. 6b also displays the diffusivities resulting from the concentration profiles recorded after a desorption step from 5 to 0 mbar (open symbols). By comparison with IR micro-imaging a (normalized) concentration of 1 is estimated to correspond to about 1.9 molecules per nm^3 [11]. The full lines in a) show the concentration profiles recalculated on the basis of the diffusivities and permeabilities shown in b) by the corresponding numerical solutions of Fick's 2nd law.

Plotting the integral of each individual profile as a function of time provides the information attainable by conventional uptake or release experiments. It is noteworthy that, for the host-guest system under consideration, the resulting uptake or release curves would represent nice examples of "disguised kinetics" [42]. In fact, analyzing the observed dependence by conventional model consideration, would suggest complete diffusion limitation, though - in reality and as directly observable with the novel options of interference and IR microscopy - overall mass transfer is also notably affected by the finite rate of surface permeation [43].

4.2. In-depth investigation of surface permeabilities

The boundaries between adjacent phases may give rise to substantial transport resistances. This is in particular true with the external surface of nanoporous particles, establishing the phase boundary between the adsorbed phase and the surrounding fluid. Textbooks dealing with the mathematics of diffusion [33] or with the role of diffusion in technological applications of nanoporous materials [44, 45] refer to this resistance, in general, as nothing more than an empirical parameters defined by the above eq. (2) since, so far, the nature of these resistances and their dependence on the relevant concentrations were beyond any experimental study.

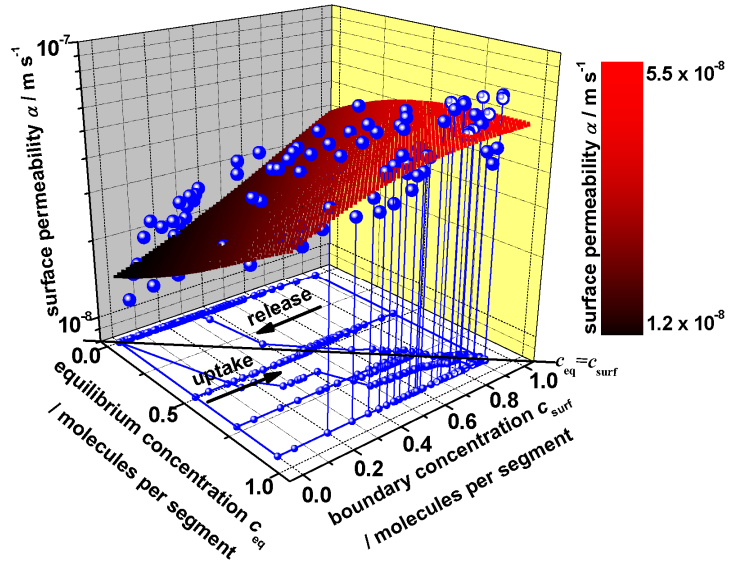


Fig. 7: First in-depth study of surface permeabilities: Permeability of propane through the external surface of a nanoporous crystal of type Zn(tbip) represented as a function of the two process-relevant concentrations, namely the equilibrium concentration as determined by the actual gas pressure and the boundary concentration at the given instant of time (data from ref.[14]). For each individual run of experiments, these concentrations are reflected by the bullets on the bottom plane. Thus, a desorption run would be reflected by a line of bullets parallel to the c_{surf} -axis, with values decreasing from the initial concentration towards the (new) equilibrium concentration. Uptake runs give rise to lines in the reversed direction, so that both of them end at the diagonal ($c_{\text{eq}} = c_{\text{surf}}$). Identical final pressures, starting from different initial pressures, lead to sequences of concentrations with one superimposed upon the other (full and open bullets in the bottom plane along line $c_{\text{eq}} \approx 0.9$). Variation of the external pressure during the experiments leads to deviations from such straight lines (two examples displayed). The plain presents the best fit of the experimental data to a function of the mean concentration $(c_{\text{surf}} + c_{\text{eq}})/2$ as a sole parameter.

With the advent of IRM and IFM and the possibility of directly monitoring the evolution of intracrystalline concentration profiles, surface permeabilities have now become accessible by direct observation. Their quantification is a prerequisite for the exploration of the mechanisms leading to finite surface permeabilities, i.e. to "surface barriers" controlling the mass exchange between the pore space and the surrounding atmosphere. While diffusivities are a function of the local concentration, permeabilities cover a total interval of concentration, namely that between the actual concentration close to the crystal surface and the equilibrium concentration. Fig. 7 displays the results of the first measurements, in which surface permeabilities have been studied as a function of these two parameters [14]. Most remarkably, in the given case the surface permeabilities are found to depend primarily on the mean concentration $(c_{\text{surf}} + c_{\text{eq}})/2$ as a sole parameter, rather than separately on c_{surf} and c_{eq} . This finding significantly facilitates the modelling

of surface resistances of nanoporous materials and, hence, the exploration of the conditions for their transport-optimized technical exploitation.

4.3. Sticking probabilities

From a microscopic point of view, the performance of nanoporous materials in molecular separation or catalytic conversion decisively depends on the penetration rate of the molecules from the surrounding atmosphere into their interior, i. e. on the probability that a molecule colliding with the external particle surface will continue its diffusion path inside of the particle [46]. With the flux through the boundary ($j_{in} = \alpha c_{eq}$) and the flux of molecules colliding with the external surface as computed by simple gas kinetics ($(2\pi RTM)^{1/2} N_A p$), with the usual notations for molecular mass and the Avogadro constant), "sticking" probabilities p_{st} may now be easily determined by simply considering the ratio between these two fluxes. Fig. 8 illustrates the way of analysis: Starting from the transient concentration profiles during molecular uptake (in particular, from the boundary values of concentration at each individual instant of time and at equilibrium, top of the figure) one determines all relevant fluxes, namely, the net flux ($j = j_{in} - j_{out}$), the flux of molecules which at each instant of time leaves the crystal ($j_{out} = \alpha c_{bound}$) and, eventually, the flux of molecules entering the crystal through the particle boundary from the external atmosphere which from the former two quantities simply results as $j_{in} \equiv j + j_{out}$. Not unexpectedly, application of this formalism yields a dramatic dependence of the sticking probability on the system under study. Neglecting, in first order approximation, any concentration dependences of the surface permeabilities, the sticking probabilities result to be of the order of 10^{-5} for methanol on the ferrierite particles under study and of more than 0.01 for isobutane on silicalite-1 [47].

Note that the present analysis is based on the assumption that mass transfer in the particles under study is exhaustively described by the eqs.(1) and (2). This means that the real host system is idealized by a homogeneous porous bulk phase of diffusivity D separated from the surrounding atmosphere by an essentially infinitely thin layer with a finite permeability α .

4.4. Transient profiles under varying boundary conditions

The development of intracrystalline concentration profiles may be recorded under conditions that are far more complex than those of the conventional uptake and release experiments. As an example, Figs. 9a and b display the evolution of intracrystalline concentration profiles in response to two pressure steps (up and down), with the second one applied before equilibration after the first one. In sorption science, this procedure is referred to as a partial-loading experiment [48]. It allows deciding about the limiting processes of molecular uptake on the basis of characteristic differences in the time dependence of desorption:

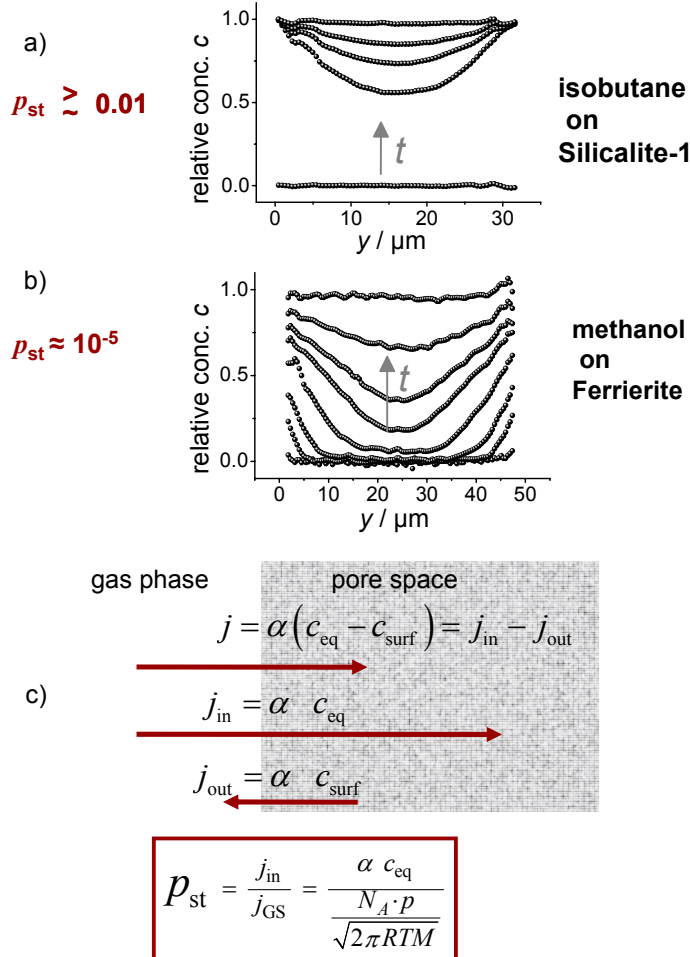


Fig. 8: Sticking probability of molecules in nanoporous materials. a) and b) transient concentration profiles of isobutane on silicalite-1 and of methanol on silica-ferrierite. c) Schematics of the fluxes. The net-flux into the pore system is the difference between the molecular flux entering and leaving the pore system. The sticking probability is the ratio between the molecular flux entering the pore space j_{in} and the molecular flux colliding with the outer crystal surface j_{GS} .

If uptake is controlled by transport resistance at the crystal surface, the intracrystalline concentration would be uniform all over the crystal already under transient uptake conditions and not only at equilibrium. This means, neglecting any concentration dependence of the transport parameters, that desorption at “partial loading”, i.e. a decrease of the external pressure before attainment of equilibrium, would lead to exactly the same time dependence of the desorption curves as under equilibrium. In the case of diffusion limitation, however, desorption at partial loading would start with concentrations enhanced close to the crystal boundary which leads to a characteristic acceleration of the desorption in its initial stage. Fig. 9b displays the intracrystalline concentration profiles in exactly this situation, revealing two characteristic transient maxima close to the crystal boundary. As a consequence of these two internal maxima, the central concentration continues to *increase* in the time interval between 1 h and (1 +

1) h, i.e. *after* a reduction of the gas pressure. It appears as if the molecules in the centre of the crystal have not yet become “aware” of the onset of desorption after 1 hour!

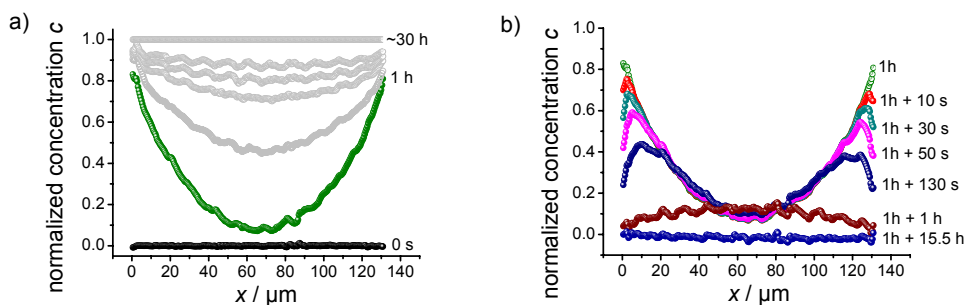


Fig. 9: Revealing transient maxima of intracrystalline concentration: Guest uptake (n-butane) by a nanoporous host ($\text{Zn}(\text{tbip})$, $0 \rightarrow 300$ mbar, a) is followed by desorption (pressure decrease to zero, b) long before equilibration (i.e. 1 h after onset of adsorption). The light grey profiles in a) show the profiles which would be recorded if the uptake process would not have been interrupted and which were in fact measured in a separate run.

5. Conclusion

With the observation of the evolution of guest profiles in nanoporous solids the optical methods of diffusion measurement, more than a century after their introduction [2], have found an attractive novel field of application. It comprises a spectrum of most diverse tasks and challenges, including the quantitation and exploration of surface permeabilities and “sticking” probabilities after collisions of the gas molecules with the surfaces of such materials and a novel type of the characterization and standardization of porous materials with respect to their transport properties, as a key criterion for their practical application.

6. Acknowledgements

We consider it both a pleasure and an obligation to refer to the input by many dear colleagues whose contributions were indispensable for the development of IFM and IRM to the present, powerful techniques of diffusion measurement. One of us (JK) acknowledges the cordial, creative atmosphere in which, already three decades ago, in Professor Harry Pfeifer’s group at the Physics Department at Leipzig University, Reinhard Danz, Jena, and Jürgen Caro, Berlin, shared his first attempts to establish IFM as an alternative to the NMR techniques for the measurement of intracrystalline diffusion in zeolites. It was only during the end of the nineties of the last century that, owing to further instrumental progress and the advent of more powerful computers, Ulf Schemmert, as part of his thesis, succeeded in the recording of the first transient concentration profiles during molecular uptake. The complications arising from single-crystal measurements, however, necessitated further substantial effort before the measurement of reproducible ad- and desorption runs with one and the same crystal have become possible. During this period of time we notably benefited from the expertise of

Douglas Ruthven, University of Maine, who stayed with us as a Humboldt Research Awardee, and of Sergey Vasenkov who came to us as a post-doc from Berkeley, California, before assuming a chair at the University of Florida, Gainesville, as well as from the diligent work of our PhD students Pavel Kortunov (now with Exxon-Mobil) and Enrico Lehmann. In our methodical development we notably profited by introducing, in parallel to IFM, the IRM technique (also referred to as IR micro-imaging) for monitoring transient intracrystalline concentration profiles. We are obliged to Hellmut Karge, Berlin, who pioneered the macro- and mesoscopic application of this technique to sorption kinetics, for many stimulating discussions and to Dhananjai B. Shah, Cleveland, and Rajamani Krishna, Amsterdam, for their involvement in the measurements and their analysis during their stays at Leipzig University within the frame of a Mercator Professorship of the German Science Foundation (DFG). Last but not least we have to thank all those colleagues who have supported us in our efforts by generously providing us with the products of the synthesis work in their groups, including Jürgen Caro (once again, now from Hannover), Jing Li (Rutgers University), Wolfgang Schmidt and Ferdi Schüth (Mülheim), Jens Weitkamp (Stuttgart) and Paul Wright (St. Andrews). It is with great sadness that we have to indicate that two of the figures who stood at the very beginning of this development, Professor Harry Pfeifer and Reinhard Danz, have recently passed away. We would like to dedicate this contribution to their memory, in deep gratitude for their sympathy, encouragement and input.

References

- [1] J. Philibert, One and a half century of diffusion: Fick, Einstein, before and beyond, in: Leipzig, Einstein, Diffusion, (J. Kärger, Eds.), Leipziger Universitätsverlag, Leipzig, 2007, p. 41 - 82.
- [2] D. Ambrosini, D. Paoletti, N. Rashidnia, *Overview of diffusion measurement by optical techniques*, Opt Laser Eng 46 (2008) 852-864.
- [3] H. Mehrer, Diffusion in Solids, Springer, Berlin, 2007.
- [4] P. T. Callaghan, Principles of NMR Microscopy, Clarendon Press, Oxford, 1991.
- [5] R. Kimmich, NMR Tomography, Diffusometry, Relaxometry, Springer, Berlin, 1997.
- [6] J. Kärger, W. Heink, *The Propagator Representation of Molecular Transport in Microporous Crystallites*, J. Magn. Reson. 51 (1983) 1-7.
- [7] R. M. Cotts, *Diffusion and Diffraction*, Nature 351 (1991) 443.
- [8] R. Valiullin, J. Karger, R. Glaser, *Correlating phase behaviour and diffusion in mesopores: perspectives revealed by pulsed field gradient NMR*, PCCP 11 (2009) 2833-2853.
- [9] M. J. Saxton, *Single-particle tracking: the distribution of diffusion coefficients*, Biophys. J. 72 (1997) 1744-1753.
- [10] A. Zürner, J. Kirstein, M. Döblingern, C. Bräuchle, T. Bein, *Visualizing single-molecule diffusion in mesoporous materials*, Nature 450 (2007) 705-709.
- [11] L. Heinke, C. Chmelik, P. Kortunov, D. M. Ruthven, D. B. Shah, S. Vasenkov, J. Kärger, *Application of interference microscopy and IR microscopy for*

- characterizing and investigating mass transport in nanoporous materials*, Chem. Eng. Tec. 30 (2007) 995-1002.
- [12] C. Chmelik, L. Heinke, J. Kärger, W. Schmidt, D. B. Shah, J. M. v. Baten, R. Krishna, *Inflection behaviour in the loading dependence of the Maxwell-Stefan diffusivity of iso-butane in MFI zeolite*, Chem. Phys. Lett 459 (2008) 141-145.
- [13] L. Heinke, D. Tzoulaki, C. Chmelik, F. Hibbe, J. M. van Baten, H. Lim, J. Li, R. Krishna, J. Kärger, *Assesing Guest Diffusivities in Porous Hosts from Transient Concentration Profiles*, Phys. Rev. Lett. 102 (2009) 065901.
- [14] D. Tzoulaki, L. Heinke, H. Lim, J. Li, D. Olson, J. Caro, R. Krishna, C. Chmelik, J. Kärger, *Assessing surface permeabilities from transient guest profiles in nanoporous host materials*, Angew. Chem. Int. Ed. 48 (2009) 3525-3528.
- [15] J. Kärger, P. Kortunov, S. Vasenkov, L. Heinke, D. B. Shah, R. A. Rakoczy, Y. Traa, J. Weitkamp, *Unprecedented Insight into Diffusion by Monitoring the Concentration of Guest Molecules in Nanoporous Host Materials*, Angew. Chem. Int. Ed. 45 (2006) 7846-7849.
- [16] H. J. V. Tyrrell, R. K. Harris, Diffusion in Liquids, Butterworth, London, 1984.
- [17] U. Schemmert, J. Kärger, J. Weitkamp, *Interference Microscopy as a Technique for Directly Measuring Intracrystalline Transport Diffusion in Zeolites*, Micropor. Mesopor. Mater. 32 (1999) 101-110.
- [18] F. Hibbe, *Interferenzmikroskopische Untersuchung der Temperaturabhängigkeit transienter Konzentrationsprofile in nanoporösen Materialien*, Diploma Thesis, University Leipzig (2008).
- [19] T. Binder, *Untersuchung des Einflusses der Realstruktur nanoporöser Materialien auf das Diffusionsverhalten von Gastmolekülen mittels Interferenzmikroskopie*, Diploma Thesis, University Leipzig (2009).
- [20] J. Kärger, R. Danz, J. Caro, *Anwendung der Interferenzmikroskopie bei der Beobachtung intrakristalliner Transportvorgänge*, Feingerätetechnik 27 (1978) 539-542.
- [21] J. Kärger, D. M. Ruthven, Diffusion in Zeolites and Other Microporous Solids, Wiley & Sons, New York, 1992.
- [22] U. Schemmert, *Interferenzmikroskopische Untersuchungen zur Moleküldiffusion in mikroporösen Materialien*, Ph.D. Thesis, University Leipzig (2001).
- [23] U. Schemmert, J. Kärger, C. Krause, R. A. Rakoczy, J. Weitkamp, *Monitoring the Evolution of Intracrystalline Concentration*, Europhys. Lett. 46 (1999) 204-210.
- [24] L. Heinke, P. Kortunov, D. Tzoulaki, M. J. Castro, P. A. Wright, J. Kärger, *Three-dimensional diffusion in nanoporous host-guest materials monitored by interference microscopy*, Europhys. Lett. 81 (2008) 26002.
- [25] P. R. Griffiths, J. A. des Haseth, Fourier Transform Infrared Spectrometry, J. Wiley & Sons, New York, 1986.
- [26] H. G. Karge, W. Niessen, H. Bludau, *In-Situ FTIR Measurements of Diffusion in Coking Zeolite Catalysts*, Appl. Catal. A 146 (1996) 339-349.

- [27] M. Hermann, H. G. Niessen, H. G. Karge, *Sorption kinetics of n-hexane in MFI-type zeolites investigated by micro-FTIR spectroscopy*, Stud. Surf. Sci. Catal. 94 (1995) 131-138.
- [28] W. Niessen, H. G. Karge, *Diffusion of p-Xylene in Single and Binary Systems in Zeolites Investigated by FTIR Spectroscopy*, Micropor. Mater. 1 (1993) 1-8.
- [29] R. J. Bell, *Introductory Fourier Transform Spectroscopy*, Academic Press, New York, 1972.
- [30] E. N. Lewis, P. J. Treado, R. C. Reeder, G. M. Story, A. E. Dowrey, C. Marcott, I. W. Levin, *Fourier-Transform Spectroscopic Imaging Using an Infrared Focal-Plane Array Detector*, Anal. Chem. 67 (1995) 3377-3381.
- [31] Y. Roggo, A. Edmond, P. Chalus, M. Ulmschneider, *Infrared hyperspectral imaging for qualitative analysis of pharmaceutical solid forms*, Anal. Chim. Acta 535 (2005) 79-87.
- [32] T. Titze, *Untersuchung des Stofftransports in nanoporösen Materialien mittels IR-Microimaging*, Diploma Thesis, University Leipzig (2009).
- [33] J. Crank, *The Mathematics of Diffusion*, Clarendon Press, Oxford, 1975.
- [34] H. G. Karge, W. Niessen, *A New Method for the Study of Diffusion and Counter Diffusion in Zeolites*, Cat. Today 8 (1991) 451-465.
- [35] M. Hermann, W. Niessen, H. G. Karge, Sorption Kinetics of n-Hexane in MFI-Type Zeolites Investigated by Micro-FTIR Spectroscopy, in: *Catalysis by Microporous Materials*, (H. K. Beyer, H. G. Karge, I. Kiricsi, J. B. Nagy, Eds.), Elsevier, Amsterdam, 1995, p. 131-138.
- [36] J. Kärger, *The random walk of understanding diffusion*, Ind. Eng. Chem. Res. 41 (2002) 3335-3340.
- [37] J. Kärger, D. Freude, *Mass transfer in micro- and mesoporous materials*, Chem. Eng. Technol. 25 (2002) 769-778.
- [38] C. Baerlocher, L. B. McCusker, D. H. Olson, *Atlas of Zeolite Framework Types*, Elsevier, Amsterdam, 2007.
- [39] R. A. Rakoczy, Y. Traa, P. Kortunov, S. Vasenkov, J. Kärger, J. Weitkamp, *Synthesis of Large Crystals of All-Silica Zeolite Ferrierite*, Micro. Mesopor. Mater. 104 (2007) 179-184.
- [40] P. Kortunov, L. Heinke, S. Vasenkov, C. Chmelik, D. B. Shah, J. Kärger, R. A. Rakoczy, Y. Traa, J. Weitkamp, *Internal concentration gradients of guest molecules in nanoporous host materials: measurement and microscopic analysis*, J. Phys. Chem. B 110 (2006) 23821-23828.
- [41] L. Pan, B. Parker, X. Huang, D. Olson, L. J.-Y., J. Li, Zn(tbip): a highly stable guest-free microporous metal organic framework with unique gas separation capability, J. Am. Chem. Soc. 128 (2006) 4180-4181.
- [42] P. Kortunov, C. Chmelik, J. Kärger, R. A. Rakoczy, D. M. Ruthven, Y. Traa, S. Vasenkov, J. Weitkamp, *Sorption kinetics and intracrystalline diffusion of methanol in ferrierite: An example of disguised kinetics*, Adsorption 11 (2005) 235-244.
- [43] L. Heinke, P. Kortunov, D. Tzoulaki, J. Kärger, *The Options of Interference Microscopy to Explore the Significance of Intracrystalline Diffusion and*

- Surface Permeation for Overall Mass Transfer on Nanoporous Materials*,
Adsorption 13 (2007) 215-223.
- [44] C. N. Satterfield, Mass Transfer in Heterogeneous Catalysis, M.I.T. Press, Cambridge, Massachusetts and London, England, 1970.
 - [45] N. Y. Chen, T. F. Degnan, C. M. Smith, Molecular Transport and Reaction in Zeolites, Wiley-VCH, New York, 1994.
 - [46] A. Jentys, R. R. Mukti, J. A. Lercher, *On the sticking probability of aromatic molecules on zeolites*, J. Phys. Chem. B 110 (2006) 17691-17693.
 - [47] L. Heinke, P. Kortunov, D. Tzoulaki, J. Kärger, *Exchange Dynamics at the Interface of Nanoporous Materials with their Surroundings*, Phys. Rev. Lett. 99 (2007) 228301.
 - [48] S. Brandani, *The partial loading ZLC Experiment*, Proc. 4th Pacific. Basin Conf. on Ads. Sci. and Tec. (2006).